Journal of Alloys and Compounds 480 (2009) 299–305

Contents lists available at ScienceDirect

Journal of Alloys and Compounds

journal homepage: www.elsevier.com/locate/jallcom

Phase equilibria on Ni–Al interface under low oxygen pressure

Chin-Guo Kuo [a], Wern Dare Jehng [b], Sheng-Jen Hsieh [c,d], Chien-Chon Chen [e,*]

[a] Department of Industrial Education, National Taiwan Normal University, Taipei 10643, Taiwan
[b] Department of Mechanical Engineering, National Chin-Yi University of Technology, Taichung 411, Taiwan
[c] Department of Engineering Technology, Texas A&M University, College Station, TX 77843-3367, United States
[d] Department of Mechanical Engineering, Texas A&M University, College Station, TX 77843-3367, United States
[e] Department of Energy and Resources, National United University, 1, Lienda, Miaoli 36003, Taiwan

ARTICLE INFO

Article history:
Received 25 November 2008
Received in revised form 14 January 2009
Accepted 24 January 2009
Available online 6 February 2009

Keywords:
Ni–Al–O
Isothermal stability diagram
Intermetallic compounds
Activity

ABSTRACT

Seventeen phases of the Ni–Al–O system at high temperatures were analyzed using thermodynamic calculations. An Ni–Al–O isothermal stability diagram was obtained from the thermochemical data. The diagram describes the interface equations for Ni/Al intermetallic compounds, Al/Al_2O_3, and Al_2O_3/Al_XNi_Y compounds, and their corresponding regions. Four univariant equilibria points and ten bivariant equilibria lines below 1126 K were obtained. The equations for the coexistence points and interface lines were also obtained. A three-domain diagram of Ni–Al–O phase arrangement at temperatures between 900 and 1191 K is shown. Thermodynamic calculations confirmed that the formation of nickel aluminate spinel ($NiAl_2O_4$) requires a threshold NiO activity ($\log a_{NiO} = -205.3/T - 0.347$) and the partial pressure of oxygen ($\log P_{O_2} = -24622/T + 8$ atm). In the Ni–Al–O system, $a_{NiO} < 0.266$ at 900 K, the compounds in the Ni/Al interface are formed in the order $Al_3Ni_{(s)} \rightarrow Al_3Ni_{2(s)} \rightarrow AlNi_{(s)} \rightarrow AlNi_{3(s)} \rightarrow Al_2O_{3(\alpha)}$. When $a_{NiO} < 0.351$ at 1911 K, the compounds in the Ni/Al interface are formed in the order $AlNi_{(s)} \rightarrow Al_2O_{3(\alpha)}$.

1. Introduction

Nickel-aluminate compounds, known as an ordered intermetallic compounds, are potential candidates for structural applications at high temperatures [1–5]. Their attractive properties include relatively low density (5.87 g/cm^3), high melting point (AlNi = 1191 K), high thermal conductivity, high specific strength, and resistance to oxidation at elevated temperatures. However, at room temperature, these materials are limited by relatively poor strength, low ductility, and the tendency to brittle fracture [6,7,11]. Many researchers [8,10,11,1,12,13] have developed processes for fabricating intermetallic compounds. These methods include mechanical alloying (MA) [8], rolling [9] and thermal contact diffusion [10].

During reactions at the interface of pure Al and Ni, the intermetallic compounds are generated in the order Al_3Ni, Al_3Ni_2, AlNi and finally $AlNi_3$. In Battezzati's investigation [9], the Ni–Al intermetallic compounds formed after Ni and Al foils were rolled. He concluded that Al_3Ni was the first phase to be observed, followed by Al_3Ni_2 and $AlNi_3$, with AlNi remaining. The oxides of Al_2O_3, NiO, and $NiAl_2O_4$ can also be formed in the Al–Ni system. Their formation depends on the partial pressure of oxygen and the activity of nickel. The mechanisms of formation of the nickel aluminate spinel ($NiAl_2O_4$) in the Ni/Al_2O_3 interfaces have been investigated in several studies [6,8–11,14,15,20–23]. Ustundag [8] found that $NiAl_2O_4$ could be formed by ball-mixing NiO and Al_2O_3 powders at high temperature, if the oxygen activity reaches a threshold value: $\log a_{O_2} > -25754/T + 7.921$. In addition, Trumble and Ruhle [15] noted that if the amount of oxygen dissolved in Ni exceeds 0.025 at.% at 1663 K, then spinel forms.

According to literature [1–11,15], several parameters – such as temperature, partial pressure of oxygen, activity of Ni, activity of compounds, Gibbs free energy, activation energy, heat treatment time, and diffusion coefficient – influence Ni/Al_2O_3 interface conditions. Consequently, researchers [1–11,15] have obtained different phases at Ni/Al_2O_3 interfaces. A convenient method of representing the thermodynamic information involves the construction of isothermal diagrams that show the range of gas compositions over which a condense phase can exit either by itself or in equilibrium with another condensed phase. This type of diagram is called an isothermal stability diagram. It can be more useful to use an isothermal stability diagram in discussing gas-condensed phases at a constant temperature rather than a general phase diagram of temperature-composition. For example, Kellogg and Basu [24], Ingraham [25], and Biswas and Davenport [26] used the isothermal stability diagram to discuss the characterizations of the Pb–S–O, Cu–S–O, and Fe–S–O systems at 1000 K.

This work considers the effect of temperature, partial oxygen pressure, activity of Ni, activity of NiO, and Gibbs free energy with reference to thermodynamic calculations for the Ni–Al–O system.

* Corresponding author. Tel.: +886 37 381836; fax: +886 37 381237.
E-mail address: chentexas@gmail.com (C.-C. Chen).

0925-8388/$ – see front matter © 2009 Elsevier B.V. All rights reserved.
doi:10.1016/j.jallcom.2009.01.118

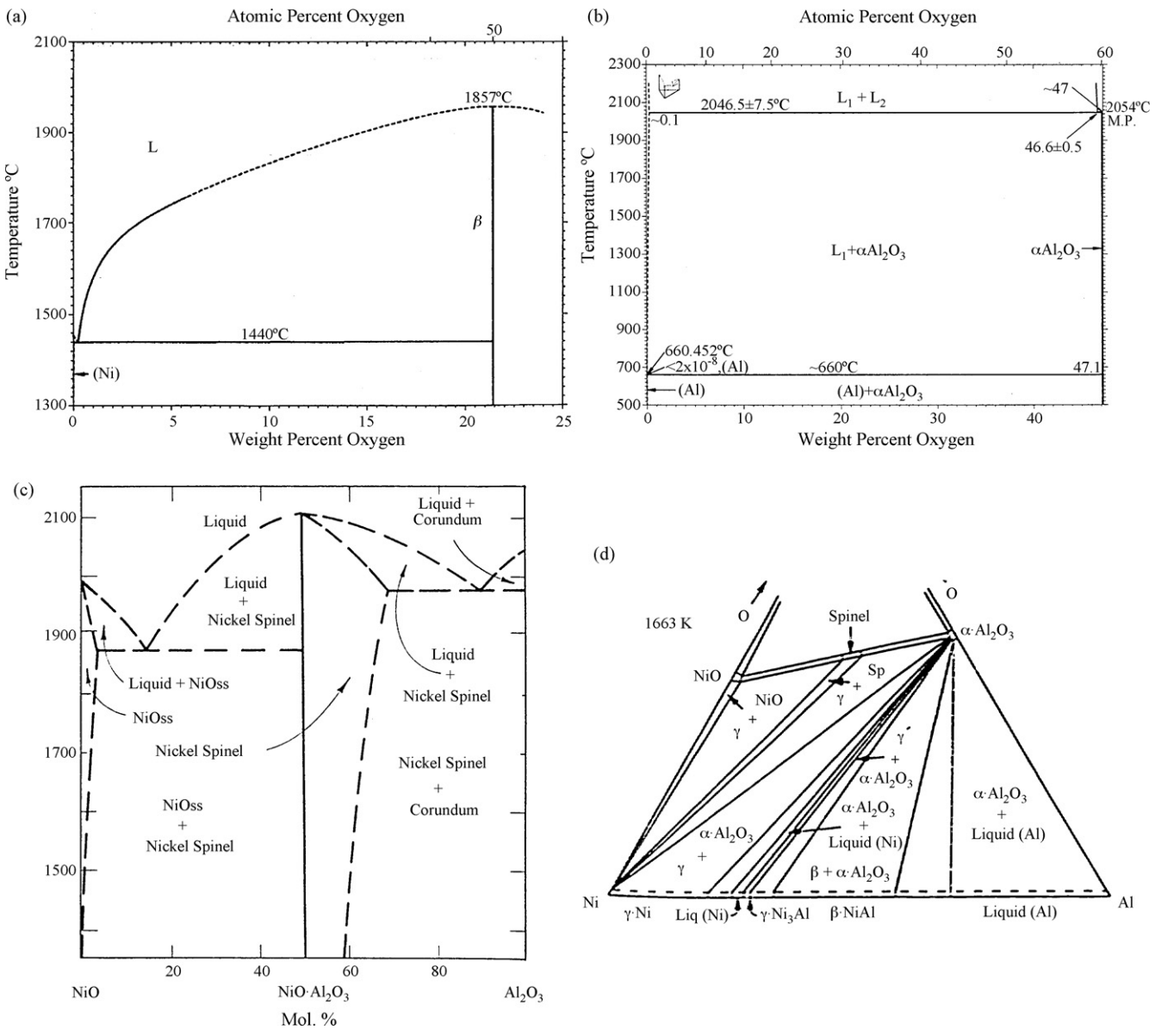

Fig. 1. Binary phase diagrams of (a) Ni–O, (b) Al–O, (c) NiO–Al_2O_3, and (d) ternary phase diagram of Ni–Al–O.

The mechanisms that operate in the Ni–Al–O system at high temperatures are thereby clarified.

2. Thermodynamic calculations and results

2.1. Phases in the Ni–Al–O system

The phase diagrams (Fig. 1) of Al–O [16], Ni–O [17], Ni–Al [18] and NiO–Al_2O_3 [19] include 12 different condensed phases and five gaseous phases. The 17 phases are, $Al_{(1/s)}$, $Al_2O_{3(\alpha)}$, $Al_2O_{3(\kappa)}$, $Al_2O_{3(\delta)}$, $Al_2O_{3(\gamma)}$, $Ai_{(s/l)}$, $AiO_{(s)}$, $AlNi_{3(s)}$, $AlNi_{(s)}$, $Al_3Ni_{2(s)}$, $Al_3Ni_{(s)}$, $NiAl_2O_{4(s)}$, $O_{2(g)}$, $Al_2O_{2(g)}$, $Al_2O_{(g)}$, $AlO_{2(g)}$ and $AlO_{(g)}$. To simplify the calculation of phases in Ni–Al–O system, the four gaseous species $Al_2O_{2(g)}$, $Al_2O_{(g)}$, $AlO_{2(g)}$ and $AlO_{(g)}$, with the exception of oxygen, will be ignored at first because of their low partial vapor pressure within the Al–O system. Moreover, because the condensed phase $Al_2O_{3(\alpha)}$ ($\Delta G = -1361.42$ kJ/mol at 1000 K) [21] is much more stable than other alumina phases ($Al_2O_{3(\kappa)}$, $Al_2O_{3(\delta)}$, $Al_2O_{3(\gamma)}$), the smallest $Al_2O_{3(\kappa)}$, $Al_2O_{3(\delta)}$, $Al_2O_{3(\gamma)}$ will also be ignored. As a result, the Ni–Al–O isothermal stability diagram will include nine condensed phases and one gaseous phase, which will be investigated by thermochemical data and thermodynamic calculations.

2.2. Gaseous species

As discussed above, gas species other than oxygen were disregarded in developing the isothermal stability diagram. However, vapor pressures in the solid and liquid phases are important in Ni–O and Al–O systems at high temperature. Therefore, this section discusses the reactions in the gas phase in Ni–O and Al–O systems. The equilibrium partial vapor pressure of nickel and oxygen in $NiO_{(s)}$ can be calculated from the Gibbs free energy as follows [21]:

$$NiO_{(s)} \rightarrow Ni_{(g)} + \tfrac{1}{2}O_{2(g)} \quad \Delta G_1^\circ = 440.2 - 0.18T\,(\text{kJ/mol}) \tag{1}$$

The standard molar free energy change ΔG_1° in this reaction is given by $\Delta G_1^\circ = -RT \ln K_1$.

K_1 can be expressed as:

$$K_1 = \frac{P_{Ni} \cdot (P_{O_2})^{0.5}}{a_{NiO}} \tag{2}$$

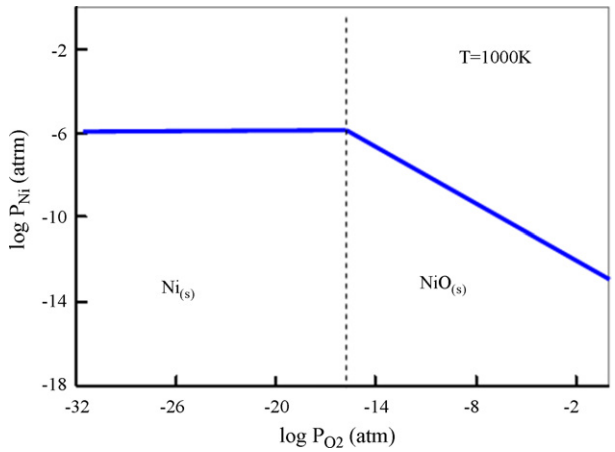

Fig. 2. Vapor pressure curve of $Ni_{(g)}$ in both condense phases of $Ni_{(s)}$ and $NiO_{(s)}$ at 1000 K.

where a_{NiO}, P_{Ni}, P_{O_2} represent the activity of NiO, partial pressure of Ni, and partial pressure of oxygen, respectively.

Since the activity of a solid is a unity, the relationship between P_{Ni} and P_{O_2} can be represented as:

$$\log P_{O_{2(g)}} = 2 \times (\log K - \log P_{Ni}) \quad (3)$$

Additionally,

$$\log K = \frac{-\Delta G_1^\circ}{2.303RT} \quad (4)$$

Based on the preceding discussion, the vapor pressures of $NiO_{(g)}$, $Ni_{(g)}$ in $Ni_{(s)}$, and $NiO_{(g)}$ in $NiO_{(s)}$ are:

$$Ni_{(s)} + \tfrac{1}{2}O_{2(g)} \rightarrow NiO_{(g)} \quad \Delta G_2^\circ = 301.9 - 0.097T\,(\text{kJ/mol}) \quad (5)$$

$$Ni_{(s)} \rightarrow Ni_{(g)} \quad \Delta G_3^\circ = 205.8 - 0.094T\,(\text{kJ/mol}) \quad (6)$$

$$NiO_{(s)} \rightarrow NiO_{(g)} \quad \Delta G_4^\circ = 536.3 - 0.18T\,(\text{kJ/mol}) \quad (7)$$

The relationships between the vapor pressures and $\log K$ are,

$$\log P_{O_{2(g)}} = 2 \times (\log P_{NiO} - \log K_1) \quad (8)$$

$$\log P_{Ni(g)} = \log K_2 \quad (9)$$

$$\log P_{NiO(g)} = \log K_3 \quad (10)$$

From Eqs. (8)–(10), the partial pressure of $NiO_{(g)}$ is much lower than that of $Ni_{(g)}$ in both $Ni_{(s)}$ and $NiO_{(s)}$ solid phases at 1000 K. The partial pressure of $Ni_{(g)}$ dominates the condensed phases $Ni_{(s)}$ and $NiO_{(s)}$, as shown in Fig. 2.

As with the Ni–O system, the reactions in the Al–O system are as follows: $Al_{(s)}/Al_{(g)}$, $Al_{(s)}/AlO_{(g)}$, $Al_{(s)}/AlO_{2(g)}$, $Al_{(s)}/Al_2O_{(g)}$, $Al_{(s)}/Al_2O_{2(g)}$, $Al_2O_{3(s)}/Al_{(g)}$, $Al_2O_{3(s)}/AlO_{(g)}$, $Al_2O_{3(s)}/AlO_{2(g)}$, $Al_2O_{3(s)}/Al_2O_{(g)}$, and $Al_2O_{3(\alpha)}/Al_2O_{2(g)}$. Fig. 3 shows the dominant gases in the Al–O system at 1000 K. When the oxygen partial pressure is lower than 10^{-47} atm, the dominant gas in the system is $Al_{(g)}$; however, if the oxygen pressure is high, the dominant gas phase changes to $AlO_{2(g)}$.

2.3. Condensed phases

Seven condensed phases ($Al_{(l/s)}$, $AlNi_{3(s)}$, $AlNi_{(s)}$, $Al_3Ni_{2(s)}$, $Al_3Ni_{(s)}$, $NiAl_2O_{4(s)}$ and $Al_2O_{3(s)}$) can be arranged on a ($\log P_{O_2} - \log a_{Ni}$) diagram of the Ni–Al–O system at constant temperature. Fig. 4 depicts the regions of each condensed phase along the axis in the ($\log P_{O_2} - \log a_{Ni}$) diagram. This so-called isothermal stability diagram is useful in estimating the relationships between each pair of condensed phases in the Ni–Al–O system; however, the

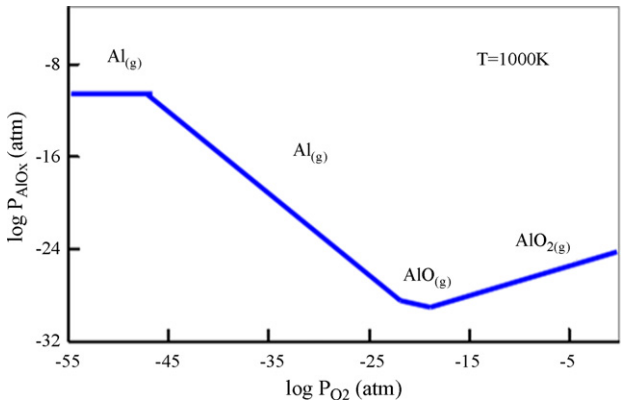

Fig. 3. Vapor pressure values of $Al_{(g)}$, $AlO_{(g)}$, and $AlO_{2(g)}$ under various oxygen pressures at 1000 K.

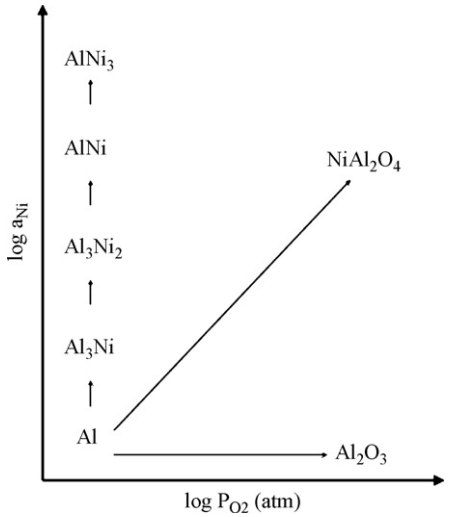

Fig. 4. Schematic diagram of Ni–Al–O compounds forming positions on the $\log a_{Ni} - \log P_{O_2}$ diagram.

interfaces between each pair of phases cannot be clearly determined from the schematic diagram. Since a couple of phases can accumulate at an interface, 36 assemblies can possibly be constructed in the $O_{(g)}$, $Ni_{(s)}$, $Al_{(l)}$, $AlNi_{3(s)}$, $AlNi_{(s)}$, $Al_3Ni_{2(s)}$, $Al_3Ni_{(s)}$, $NiAl_2O_{4(s)}$ and $Al_2O_{3(s)}$ phases—such as $Al_{(l)}/Al_2O_{3(s)}$, $Al_{(l)}/AlNi_{3(s)}$, $AlNi_{3(s)}/Al_2O_{3(s)}$, $AlNi_{3(s)}/Al_3Ni_{2(s)}$. However, as shown in Fig. 4, no interfaces of Al/Al_3Ni_2, Al/AlNi, $Al/AlNi_3$, $Al_3Ni/AlNi$, $Al_3Ni/AlNi_3$/or $Al_3Ni_2/AlNi_3$ were found. Therefore, 36 terms, except those associated with these 6 non-existing interfaces, exist as shown in Fig. 5. Nevertheless, there still is a problem of overlapping in the Al_2O_3

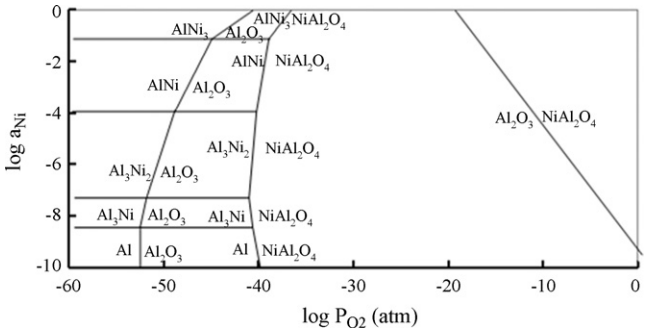

Fig. 5. Condensed phases of Ni–Al–O compound regions on the $\log a_{Ni} - \log P_{O_2}$ diagram in Ni–Al–O isothermal stability diagram at 900 K.

Table 1
Reactions and Gibbs free energies of possible compounds forming at Al–Ni interface under oxygen pressure in temperature range from 800 to 2000 K.

No.	Reactions	ΔG (kJ/mol)
1	$NiAl_2O_4 \rightarrow Ni + \frac{1}{2}O_2 + Al_2O_3$	$2.35.7 - 0.08T$
2	$\frac{3}{2}Al_2O_3 + 2Ni \rightarrow Al_3Ni_2 + \frac{9}{4}O_2$	$40501.2 - 0.4T$
3	$Al_2O_3 + 6Ni \rightarrow 2AlNi_3 + \frac{3}{2}O_2$	$1344.2 - 0.27T$
4	$\frac{3}{2}Al_2O_3 + Ni \rightarrow Al_3Ni + \frac{9}{4}O_2$	$2343.9 - 0.45T$
5	$Al_2O_3 + 2Ni \rightarrow 2AlNi + \frac{3}{2}O_2$	$1415.1 - 0.28T$
6	$Al_3O_2 + \rightarrow Al_3Ni + Ni$	$140.7 - 0.02T$
7	$Al_3Ni_2 + Ni \rightarrow 3AlNi$	$-78.7 + 0.01T$
8	$AlNi_3 \rightarrow AlNi + 2Ni$	$37.3 - 0.005T$
9	$2Al + \frac{3}{2}O_2 \rightarrow Al_2O_3$	$-1692.5 + 0.33T$
10	$3Al + Ni \rightarrow Al_3Ni$	$-190.8 + 0.05T$

and $NiAl_2O_4$ regions. Thus, several other interfaces do not exist, and should be deleted from the 36 terms. The interfaces $Al/NiAl_2O_4$, $Al_3Ni/NiAl_2O_4$, $Al_3Ni_2/NiAl_2O_4$, $AlNi/NiAl_2O_4$, and $AlNi_3/NiAl_2O_4$ must be erased to label compound's domains in Fig. 5. Finally, only twelve coexistence terms were retained from the original terms. Table 1 presents the standard and obtained Gibbs free energy of the twelve coexistence terms.

Combining Figs. 4 and 5 with the thermodynamic data from Table 1 yields the interfaces of both compounds as shown in Fig. 6. For example, to estimate the boundaries of the Al_3Ni_2 region, first, reactions (11)–(13) and their Gibbs free energy of formation are obtained from Table 1. Second, the relationship between the activity of Ni and the oxygen partial pressure is obtained from reaction (11), under the Al_3Ni_2/Al_2O_3 coexistence condition. Third, the activity of Ni is calculated from reaction (12) under the $Al_3Ni_2/AlNi$ coexistence condition. Finally, reaction (13) can also be used to calculate the activity of Ni under the Al_3Ni_2/Al_3Ni coexistence condition.

$$\frac{3}{2}Al_2O_3 + 2Ni \rightarrow Al_3Ni_2 + \frac{9}{4}O_2 \quad (11)$$

$$Al_3Ni_2 + Ni \rightarrow 3AlNi \quad (12)$$

$$Al_3Ni_2 \rightarrow Al_3Ni + Ni \quad (13)$$

Additionally, the oxygen pressure obtained from reaction (11) is:

$$\log P_{O_2} = \frac{4}{9}(\log K + 2\log a_{Ni}) \quad (14)$$

An oblique line E in Fig. 6 can be drawn along the axis in the $\log P_{O_2} - \log a_{Ni}$ diagram. The line represents the interface between Al_2O_3 and Al_3Ni_2. Restated, the activity of Ni between AlNi and Al_3Ni_2 can be determined from reaction (12) as follows:

$$\log a_{Ni} = \log K_{(Al_3Ni_2/AlNi)} \quad (15)$$

Therefore, in Fig. 6, line F (the interface between Al_3Ni_2 and AlNi) is determined by reaction (15) and line D (interface between Al_3Ni_2 and Al_3Ni) is determined from reaction (13); lines D, E, and F define the Al_3Ni_2 region. Accordingly, in Fig. 6, the regions associated with the other compounds can also be determined, and then the equations of univariant equilibria (triple-phase coexistence) points and bivariant equilibria (two-phase coexistence) lines can be calculated, as shown in Tables 2 and 3.

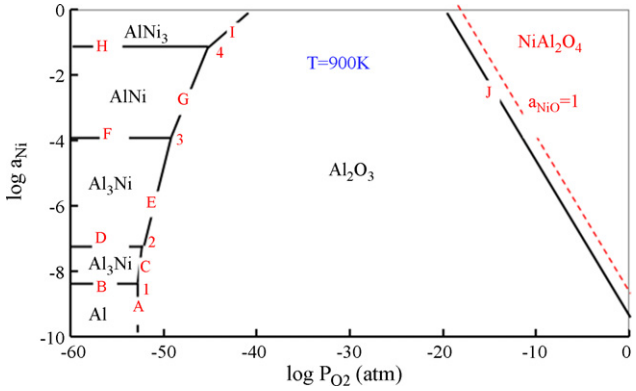

Fig. 6. Two phase coexistence lines and triple points of Ni–Al–O compounds on the $\log a_{Ni} - \log P_{O_2}$ diagram in Ni–Al–O isothermal stability diagram at 900 K.

Table 2
Reactions and Gibbs free energies of Ni–Al–O system on univariant equilibria points in temperature range from 900 to 1126 K.

No.	Reaction	ΔG (kJ/mol)
1	$Al_2O_3 + Al + Ni \rightarrow Al_3Ni + \frac{3}{2}O_2$	$1501.7 - 0.28T$
2	$3Al_2O_3 + 3Ni \rightarrow Al_3Ni + Al_3Ni_2 + \frac{9}{2}O_2$	$4553.1 - 0.87T$
3	$2Al_2O_3 + 3Ni \rightarrow AlNi + Al_3Ni_2 + 3O_2$	$2915.1 - 0.57T$
4	$Al_2O_3 + 4Ni \rightarrow AlNi + AlNi_3 + \frac{3}{2}O_2$	$1380.9 - 0.27T$

Table 3
Reactions and Gibbs free energies of Ni–Al–O system on bivariant equilibria lines in temperature range from 900 to 1126 K.

No.	Reaction	ΔG (kJ/mol)
A	$2Al + \frac{3}{2}O_2 \rightarrow Al_2O_3$	$-1692.1 + 0.33T$
B	$3Al + Ni \rightarrow Al_3Ni$	$-190.8 + 0.05T$
C	$\frac{3}{2}Al_2O_3 + Ni \rightarrow Al_3Ni + \frac{9}{4}O_2$	$2347.3 - 0.44T$
D	$Al_3Ni_2 \rightarrow Al_3Ni + Ni$	$141.4 - 0.02T$
E	$\frac{3}{2}Al_2O_3 + 2Ni \rightarrow Al_3Ni_2 + \frac{9}{4}O_2$	$2205.8 - 0.43T$
F	$Al_3Ni_2 + Ni \rightarrow 3AlNi$	$-77.9 + 0.01T$
G	$Al_2O_3 + 2Ni \rightarrow 2AlNi + \frac{3}{2}O_2$	$1418.6 - 0.28T$
H	$AlNi_3 \rightarrow AlNi + 2Ni$	$37.7 - 0.005T$
I	$Al_2O_3 + 6Ni \rightarrow 2AlNi_3 + \frac{3}{2}O_2$	$1343.2 - 0.03T$
J	$NiAl_2O_4 \rightarrow Al_2O_3 + Ni + \frac{1}{2}O_2$	$235.7 - 0.08T$

2.4. Temperatures from 900 to 1911 K

Different intermetallic compounds in an Ni–Al system have different melting points. By drawing a 3-D (axes temperature, $\log P_{O_2}$, $\log a_{Ni}$) isothermal stability diagram, the melting point of each intermetallic compound must first be determined; for example Al_3Ni = 1127 K, Al_3Ni_2 = 1406 K, $AlNi_3$ = 1658 K and AlNi = 1911 K. Second, the equation of triple-phase coexistence point must be set up. Finally, a line is drawn between the higher melting point compound and the lower melting point compound. Fig. 7 shows an isothermal stability diagram in which 1127 K is the melting point of Al_3Ni and T_t is the triple-phase coexistence point (Al, Al_3Ni, Al_2O_3 univariant point). The equation for the point of coexistence is as

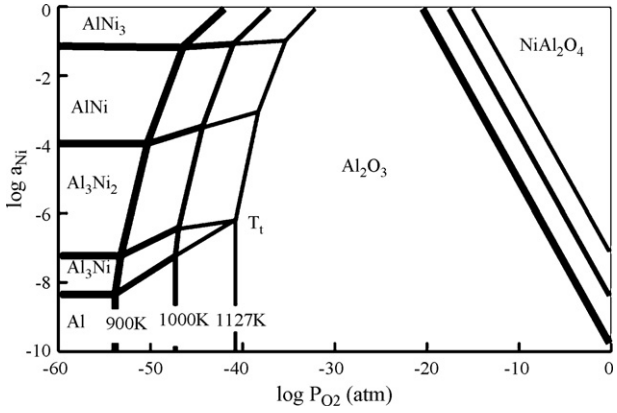

Fig. 7. Isothermal stability diagram of Ni–Al–O compounds in temperature range from 900 to 1127 K, in which 1127 K is the melting point of Al_3Ni and T_t is the triple-phase coexistence point (Al, Al_3Ni, Al_2O_3 univariant point).

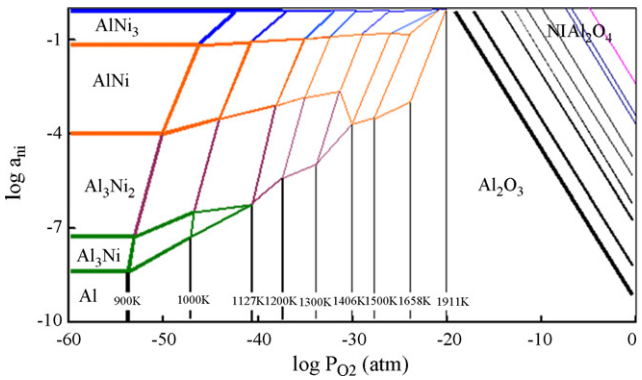

Fig. 8. Isothermal stability diagram of Ni–Al–O compounds in temperature range from 900 to 1911 K under various oxygen pressures and Ni activity values.

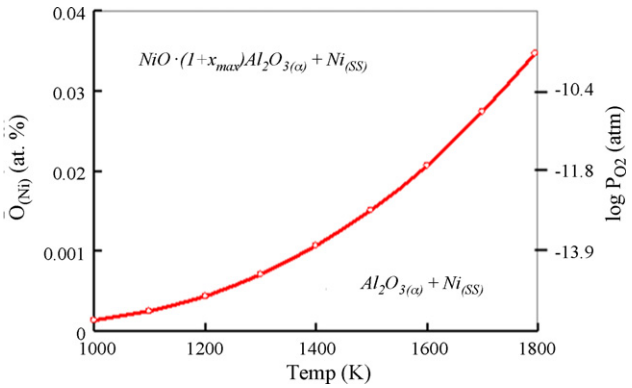

Fig. 9. Solubility line of oxygen atoms in Ni under various oxygen pressures in temperature range from 1000 to 1800 K.

follows:

$$Al_2O_{3(\alpha)} + Al_{(l)} + Ni_{(s)} \rightarrow Al_3Ni_{(s)} + \tfrac{3}{2}O_{2(g)}$$

$$\Delta G^\circ = 1501.7 - 0.28T\,(\mathrm{kJ/mol}) \quad (16)$$

In Fig. 8, the temperature range is widened from 900 to 1191 K. The diagram clearly shows regions for Al_3Ni, Al_3Ni_2, $AlNi_3$, AlNi, Al_2O_3, Al and $NiAl_2O_4$ at various temperatures.

3. Discussion

3.1. Sorting compounds by Gibbs free energy of formation

The thermodynamic stabilities of compounds in a Ni–Al–O system were evaluated by considering their Gibbs free energy. In a Ni–Al–O system, in ascending order of Gibbs free energy, the compounds at 1000 K are:

$$NiAl_2O_{4(s)} \rightarrow Al_2O_{3(\alpha)} \rightarrow Al_2O_{3(\kappa)} \rightarrow Al_2O_{3(\delta)} \rightarrow Al_2O_{3(\gamma)} \rightarrow Al_2O_{2(g)} \rightarrow Al_3Ni_{2(s)} \rightarrow NiO_{(s)} \rightarrow Al_2O_{(g)} \rightarrow AlO_{2(g)} \rightarrow AlNi_{3(s)} \rightarrow Al_3Ni_{(s)} \rightarrow AlNi_{(s)} \rightarrow AlO_{(g)}.$$

Thus, spinel ($NiAl_2O_4$) is the most stable phase and $AlNi_{(s)}$ is less stable than the other intermetallic compounds. In the Ni–Al–O isothermal stability diagram, the activity of NiO is a given condition; alumina in κ, δ, γ phases and gas phases was neglected. Therefore, the order is:

$$NiAl_2O_{4(s)} \rightarrow Al_2O_{3(\alpha)} \rightarrow Al_3Ni_{2(s)} \rightarrow AlNi_{3(s)} \rightarrow Al_3Ni_{(s)} \rightarrow AlNi_{(s)}.$$

In conclusion, the order of formation of Ni–Al–O intermetallic compounds can be determined from thermodynamics. The AlNi phase was the last to appear.

3.2. Equations for spinel formation and the threshold of NiO activity

Five different equations for the formation of spinel are,

$$Ni_{(s)} + Al_2O_{3(\alpha)} \rightarrow NiAl_2O_{4(s)} \quad (\Delta G = 328.4 - 0.035T\,(\mathrm{kJ/mol})) \quad (17)$$

$$Ni_{(s)} + \tfrac{4}{3}Al_2O_{3(\alpha)} \rightarrow NiAl_2O_{4(s)} + \tfrac{2}{3}Al_{(l)} \quad (\Delta G = 328.4 - 0.035T\,(\mathrm{kJ/mol})) \quad (18)$$

$$2Al_{(l)} + 4NiO_{(s)} \rightarrow NiAl_2O_{4(s)} + 3Ni_{(s)} \quad (\Delta G = -1000 + 0.075T\,(\mathrm{kJ/mol})) \quad (19)$$

$$Ni_{(s)} + \tfrac{1}{2}O_{(g)} + Al_2O_{3(\alpha)} \rightarrow NiAl_2O_{4(s)} \quad (\Delta G = -2159.5 + 0.49T\,(\mathrm{kJ/mol})) \quad (20)$$

$$Ni_{(s)} + \underline{O}_{Ni} + Al_2O_{3(\alpha)} \rightarrow NiO \cdot Al_2O_{3(\alpha)} \quad (\Delta G = -62800.2 + 7.1T\,(\mathrm{kJ/mol})) \quad (21)$$

Eq. (17) is a general form of the spinel forming equation in the phase diagram and literature [1–5]; moreover, the Gibbs free energy of formation of spinel is very low (−1520.6 kJ/mol at 1000 K), and so the reaction represents possible formation of spinel. However, the Gibbs free energy of reaction (18) is too high (293.43 kJ/mol at 1000 K). Hence, this equation cannot describe the formation of spinel. Despite the fact that the Gibbs free energy of Eq. (19) is negative and low (−925 kJ/mol at 1000 K), it is also an unfeasible equation since the partial pressure of oxygen at which alumina is formed ($10^{-47.4}$ atm at 1000 K) and the Gibbs free energy (−1361.05 kJ/mol at 1000 K) of the formation of alumina are lower than in NiO. Therefore, in the Al/NiO interface, Al_2O_3 may form when NiO decomposes at high temperature. Restated, if Al oxidizes to Al_2O_3 first, then the reaction becomes that described by reaction (20), in which the Gibbs free energy is lower than that of reaction (19). Therefore, reaction (20) is more feasible than reaction (19). With reference to reaction (20), the oxygen partial pressure of the decomposition of Al_2O_3 and NiO is $10^{-47.4}$ and $10^{-15.5}$ atm, respectively, at 1000 K according to Table 1. If the partial pressure of oxygen in the system is between $10^{-47.4}$ and $10^{-15.5}$ atm, then Al oxidizes to alumina, and Ni does not oxidize to NiO. Therefore, reaction (20) is feasible.

Trumble and Ruhle [15] stated that when $\log a_{O_2} > -25754/T + 7.921$, reaction (21) is a possible equation for the formation of spinel. The solubility of oxygen in Ni is given in Eq. (22), where e°_O and e°_{Ni} are interaction coefficients for Ni/O alloy, and %$\underline{O}$ is the mass solubility (wt.%) of oxygen in the Ni matrix.

$$(e^\circ_O \cdot \%\underline{O} + e^\circ_{Ni} \cdot \%\underline{Ni}) + \log \%\underline{O} = -\log K \quad (22)$$

Fig. 9 illustrates Eq. (22). According to the preceding discussion, the possible equations for the formation of spinel are reactions (17), (20) and (21). Now consider again the order: $NiAl_2O_{4(s)} \rightarrow Al_2O_{3(\alpha)} \rightarrow Al_3Ni_{2(s)} \rightarrow AlNi_{3(s)} \rightarrow Al_3Ni_{(s)} \rightarrow AlNi_{(s)}$. In reactions (17), (20) and (21), Al_2O_3 forms before spinel. Therefore, the order must should be corrected to: $Al_2O_{3(\alpha)} \rightarrow NiAl_2O_{4(s)} \rightarrow Al_3Ni_{2(s)} \rightarrow AlNi_{3(s)} \rightarrow Al_3Ni_{(s)} \rightarrow AlNi_{(s)}$. When the temperature is 1000 K, aluminum is in the liquid phase but nickel is in the solid phase so, liquid rich-phase compounds can form more easily than solid rich-phase compounds. Thus, $Al_3Ni_{(s)}$ should be sequenced behind spinel. The order is:

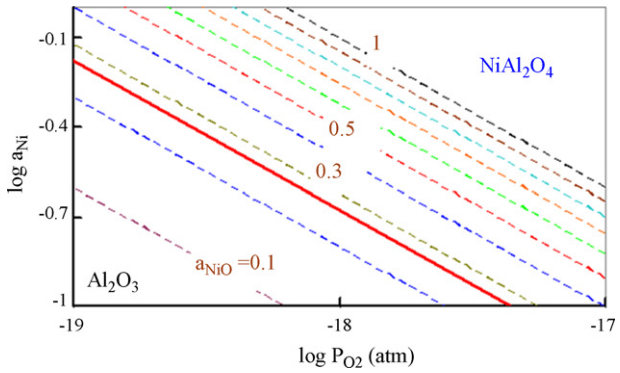

Fig. 10. Diagram of two phases (Al_2O_3 and $NiAl_2O_4$). The line coexists when the activity of NiO is 0.266 at 900 K.

$Al_2O_{3(\alpha)} \rightarrow NiAl_2O_{4(s)} \rightarrow Al_3Ni_{(s)} \rightarrow Al_3Ni_{2(s)} \rightarrow AlNi_{3(s)} \rightarrow AlNi_{(s)}$.

In reaction (17), the NiO activity is a unity. If the oxygen partial pressure is too low, NiO may decompose, causing its activity to vary away from unity. Fig. 10 shows that spinel decomposes at 900 K when the activity of NiO is below 0.266. Fig. 11 shows the effect of the activity of NiO in the stable and decomposition regions of spinel at 900 K. The equation of the curve in Fig. 11 is:

$$\log a_{NiO} = -0.347 - \frac{205.3}{T} \quad (23)$$

3.3. Ni–Al intermetallic compounds

The activity of NiO and oxygen partial pressure controls the stability of NiO and $NiAl_2O_4$, as shown in reactions (24) and (25).

$$Ni_{(s)} + \tfrac{1}{2}O_{2(g)} \rightarrow NiO \quad \Delta G = -234.5 + 0.09T \text{ kJ/mol} \quad (24)$$

$$Ni_{(s)} + \tfrac{1}{2}O_{2(g)} + Al_2O_{3(\alpha)} \rightarrow NiAl_2O_{4(s)}$$
$$\Delta G = -235.7 + 0.08T \text{ kJ/mol} \quad (25)$$

In reaction (25), when $a_{NiO} > 0.266$ and $\log P_{O_2} > -10^{-18.31}$ atm at 900 K, NiO and $NiAl_2O_4$ are stable. Therefore, the multi-layers in the Al/Ni interfaces are as follows: $Al_{(l)}$/$Al_3Ni_{(s)}$/$Al_3Ni_{2(s)}$/$AlNi_{(s)}$/$AlNi_{3(s)}$/$Al_2O_{3(s)}$/$NiAl_2O_{4(s)}$/$NiO_{(s)}$/$Ni_{(s)}$. In contrast, when $a_{NiO} > 0.266$ and $\log P_{O_2} < 10^{-18.31}$ atm at 900 K, NiO and $NiAl_2O_4$ were decomposed. So the interfaces were $Al_{(l)}$/$Al_3Ni_{(s)}$/$Al_3Ni_{2(s)}$/$AlNi_{(s)}$/$AlNi_{3(s)}$/$Al_2O_{3(s)}$/$Ni_{(s)}$. Various elements and compounds present in the Al–Ni interfaces depend on a_{NiO} and P_{O_2} conditions at various temperatures, as shown in Table 4. Results presented in Table 4 show that high temperature, low oxygen pressure, and low NiO activity are the possible conditions for obtaining AlNi and $AlNi_3$ phases.

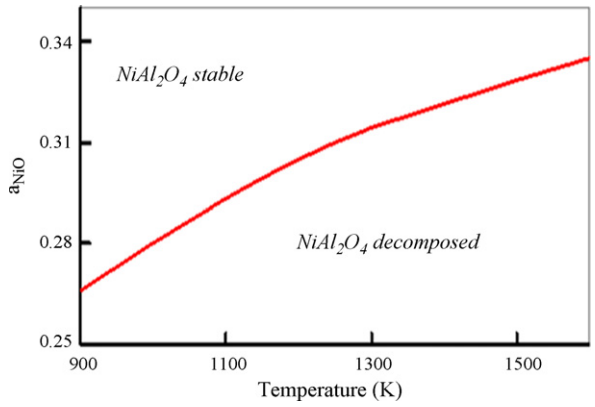

Fig. 11. Decomposition curve of spinel ($NiAl_2O_4$) with varying NiO activity at 900 K.

Table 4
Compounds forming on Al–Ni interface under various NiO activity conditions, oxygen partial pressures and temperatures.

Temperature (K)	Conditions	Interfaces
900	$a_{NiO} < 0.266$ $\log P_{O_2} < -18.31$	$Al_{(l)}/Al_3Ni_{(s)}/Al_3Ni_{2(s)}/AlNi_{(s)}/AlNi_{3(s)}/Al_2O_{3(s)}/Ni_{(s)}$
1128	$a_{NiO} < 0.295$ $\log P_{O_2} < -12.83$	$Al_{(l)}/Al_3Ni_{2(s)}/AlNi_{(s)}/AlNi_{3(s)}/Al_2O_{3(s)}/Ni_{(s)}$
1407	$a_{NiO} < 0.321$ $\log P_{O_2} < -8.52$	$Al_{(l)}/AlNi_{(s)}/Al_3Ni_{(s)}/Al_2O_{3(s)}/Ni_{(s)}$
1659	$a_{NiO} < 0.338$ $\log P_{O_2} < -5.87$	$Al_{(l)}/AlNi_{(s)}/Al_2O_{3(s)}/Ni_{(s)}$
1912	$a_{NiO} < 0.351$ $\log P_{O_2} < -3.92$	$Al_{(l)}/Al_2O_{3(s)}/Ni_{(s)}$

4. Conclusions

Thermodynamic calculations were performed to estimate Ni/Al interface reactions under various partial oxygen pressure and activity of nickel conditions in a Ni–Al–O system. Solid, liquid and gas phases in the Ni–Al–O system were analyzed using thermochemical data and phase diagrams. Seven condensed phases ($Al_{(l)}$, $AlNi_{3(s)}$, $AlNi_{(s)}$, $Al_3Ni_{2(s)}$, $Al_3Ni_{(s)}$, $NiAl_2O_{4(s)}$ and $Al_2O_{3(s)}$) were arranged along an axis of ($\log P_{O_2}$ – $\log a_{Ni}$ – temperature) 3-domains diagram. The compounds forming in the Ni/Al interface were dependent on the temperature, activity of NiO, and partial oxygen pressure. When $a_{NiO} > 0.266$ and $\log P_{O_2} > -10^{-18.31}$ atm at 900 K, the multi-layers in the Al/Ni interfaces were: $Al_{(s)}$/$Al_3Ni_{(s)}$/$Al_3Ni_{2(s)}$/$AlNi_{(s)}$/$AlNi_{3(s)}$/$Al_2O_{3(s)}$/$NiAl_2O_{4(s)}$/$NiO_{(s)}$/$Ni_{(s)}$. When $a_{NiO} < 0.266$ and $\log P_{O_2} < 10^{-18.31}$ atm at 900 K, the interfaces were $Al_{(s)}$/$Al_3Ni_{(s)}$/$Al_3Ni_{2(s)}$/$AlNi_{(s)}$/$AlNi_{3(s)}$/$Al_2O_{3(s)}$/$Ni_{(s)}$. When $a_{NiO} < 0.351$ at 1911 K, the compounds in the Al/Ni interface formed in the following order: $Al_{(l)}/AlNi_{(s)}/Al_2O_{3(\alpha)}/Ni_{(s)}$. A 3-D diagram of Ni–Al–O isothermal stability was constructed over the temperature range from the melting point of Al to the melting point of AlNi. This diagram is useful for determining accurate areas of $NiAl_2O_4$, Al, Al_2O_3 and Ni/Al intermetallic compounds in the Ni–Al–O system. In Ni/Al systems, AlNi and $AlNi_3$ have favorable properties at elevated temperatures. According to thermodynamic calculations, low oxygen pressure, high temperature, and low NiO activity promote the formation of AlNi and $AlNi_3$ phases.

References

[1] D. Padmavardhani, A. Gomez, Intermetallics 6 (1998) 229.
[2] D.F. Susan, W.Z. Misiolek, Metall. Mater. Trans. A 32A (2001) 379.
[3] H. Doty, R. Abbaschian, Mater. Sci. Eng. A195 (1995) 101.
[4] H.X. Zhu, R. Abbaschian, Mater. Sci. Eng. A282 (2000) 1.
[5] H.X. Zhu, R. Abbaschian, Composites B31 (2000) 83.
[6] T. Fujimura, S.I. Tanaka, Acta Mater. 45 (1997) 491.
[7] C.M. Ward, R. Minor, Intermetallics 4 (1995) 217.
[8] E. Ustundag, R. Subramanian, Acta Metall. Mater. 43 (1995) 383.
[9] L. Battezzati, P. Pappalepore, Acta Metall. Mater. 47 (1999 1901).
[10] J.L. Lieblich, C. Gonzalez, Intermetallics 5 (1997) 515.
[11] Chung-Kwei Lin, Shi-Shen Hong, Intermetallics 8 (2000) 1043.
[12] W.H. Tuan, W.B. Chou, Mater. Chem. Phys. 56 (1998) 157.
[13] A.J. Steven, M.B. James, Mater. Lett. 19 (1994) 233.
[14] H. Doty, R. Abbaschian, Mater. Sci. Eng. A 195 (1995) 101.
[15] K.P. Trumble, M. Ruhle, Acta Metall. Mater. 39 (1991) 1915.
[16] Westerville, Diagrams for Ceramists, American Ceramic Society, *Columbus, Ohio*, 1990, p. 144.
[17] Thaddeus B. Massalski (Ed.), American Society for Metals, OH, U.S.A., 1992, p. 2.49.
[18] Thaddeus B. Massalski (Ed.), American Society for Metals, OH, U.S.A., 1992, p. 2.312.
[19] Westerville, Diagrams for Ceramists, American Ceramic Society, *Columbus, Ohio*, 1990, p. 90.
[20] Chen Ti Hu, Wen Chih Chiou, Metall. Trans. B 29B (1998) 1069.

[21] M.W. Chase Jr., C.A. Davies, J.R. Davies, Jr., D.J. Fulrip, R.A. McDonald, and A.N. Syverud, Journal of Physical and Chemical Reference Data, third ed., American Chemical Society, New York, 1985.
[22] F. Sauert, E. Schultze-Rhonhof, Thermochemical data of pure substances, second ed., Weinheim, Federal Republic of Germany, New York, 1993.
[23] M. Atzmon, Phys. Rev. Lett. 64 (1990) 487.
[24] H.H. Kellogg, S.K. Basu, Trans. Met. Soc. AIME 218 (1960) 70.
[25] T.R. Ingraham, Trans. Met. Soc. AIME 233 (1965) 359.
[26] A.K. Biswas, W.G. Davenport, Extractive Metallurgy of Copper, 2nd ed., Pergamon Press, New York, 1980.